HHS Public Access

Author manuscript

Addict Biol. Author manuscript; available in PMC 2023 March 01.

Published in final edited form as:

Addict Biol. 2022 March ; 27(2): e13134. doi:10.1111/adb.13134.

Repeated blast mild traumatic brain injury and oxycodone self-administration produce interactive effects on neuroimaging outcomes

Matthew J. Muelbl, B.S.[1,3], **Breanna L. Glaeser, B.A.**[1,3], **Alok S. Shah, M.S.**[4,5], **Rachel A. Chiariello, B.A.**[4,5], **Natalie N. Nawarawong, Ph.D.**[1,3,6], **Brian D. Stemper, Ph.D.**[2,3,4,5], **Matthew D. Budde, Ph.D.**[3,4,5], **Christopher M. Olsen, Ph.D.**[1,3,4,*]

[1]Department of Pharmacology and Toxicology, Medical College of Wisconsin, 8701 Watertown Plank Rd., Milwaukee, WI 53226, USA;

[2]Joint Department of Biomedical Engineering, Marquette University, 1515 W. Wisconsin Ave, Milwaukee WI, 53233, USA and Medical College of Wisconsin, 8701 Watertown Plank Rd., Milwaukee, WI 53226, USA;

[3]Neuroscience Research Center, Medical College of Wisconsin, 8701 Watertown Plank Rd., Milwaukee, WI 53226, USA;

[4]Department of Neurosurgery, Medical College of Wisconsin, 8701 Watertown Plank Rd., Milwaukee, WI 53226, USA;

[5]Clement J. Zablocki Veterans Affairs Medical Center, 5000 W National Ave, Milwaukee, WI 53295, USA;

[6]Deparment of Pharmacology & Toxicology, University of Texas at Austin

Abstract

Traumatic brain injury (TBI) and drug addiction are common comorbidities, but it is unknown if the neurological sequelae of TBI contribute to this relationship. We have previously reported elevated oxycodone seeking after drug self-administration in rats that received repeated blast TBI (rbTBI). TBI and exposure to drugs of abuse can each change structural and functional neuroimaging outcomes, but it is unknown if there are interactive effects of injury and drug exposure. To determine the effects of TBI and oxycodone exposure, we subjected rats to rbTBI and oxycodone self-administration and measured drug seeking and several neuroimaging measures. We found interactive effects of rbTBI and oxycodone on fractional anisotropy (FA) in the nucleus accumbens (NAc), and that FA in the medial prefrontal cortex (mPFC) was correlated with drug seeking. We also found an interactive effect of injury and drug on widespread functional

[*]Corresponding author: Christopher M. Olsen, PhD, Medical College of Wisconsin, 8701 Watertown Plank Road, Milwaukee, WI 53226, USA, Phone: (414) 955-7629, colsen@mcw.edu.

Author Contributions

BDS, MDB, and CMO were responsible for the study concept and design. MJM, BLG, and NNN contributed to the acquisition of behavioral data. ASS and RAC conducted the injury model. NNN, BDS, MDB, and CMO assisted with data analysis and interpretation of findings. MJM, BLG, BDS, MDB, and CMO drafted the manuscript. All authors critically reviewed content and approved final version for publication.

Disclosure/Conflict of Interest

The authors declare no conflict of interest. Data available on request from the authors.

connectivity and regional homogeneity of the blood oxygen level dependent (BOLD) response, and that intra-hemispheric functional connectivity in the infralimbic medial prefrontal cortex positively correlated with drug seeking. In conclusion, rbTBI and oxycodone self-administration had interactive effects on structural and functional magnetic resonance imaging (MRI) measures, and correlational effects were found between some of these measures and drug seeking. These data support the hypothesis that TBI and opioid exposure produce neuroadaptations that contribute to addiction liability.

Graphical Abstract

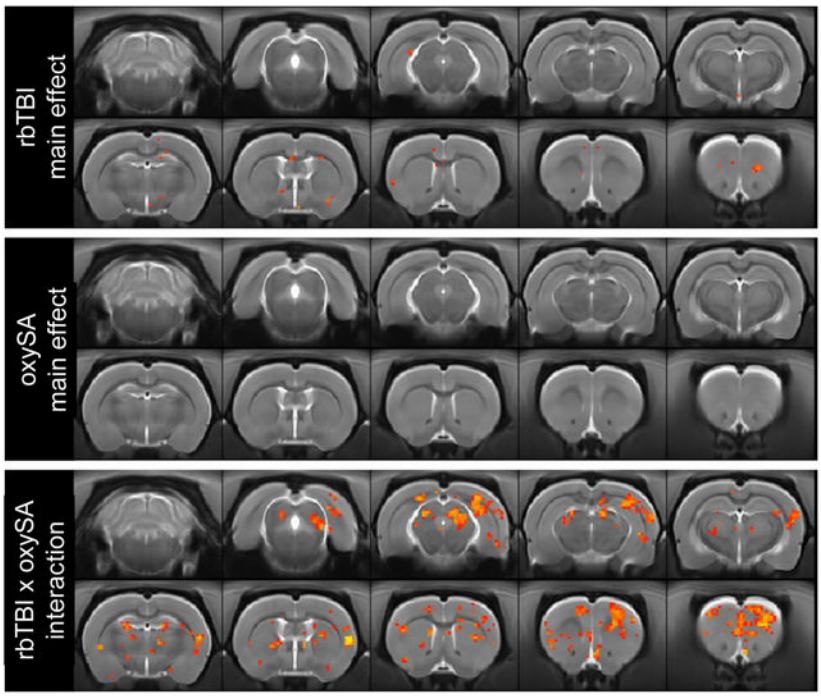

We previously found that repeated blast traumatic brain injury (rbTBI) increases oxycodone seeking after self-administration. Here, we report that rbTBI and oxycodone self-administration have interactive effects on structural and functional neuroimaging measures. Fractional anisotropy negatively correlated with drug seeking in the prelimbic and infralimbic prefrontal cortex, and interhemispheric connectivity of the infralimbic prefrontal cortex positively correlated with drug seeking.

Keywords

drug seeking; extinction; MRI; opioid; traumatic brain injury

Introduction

Traumatic brain injury (TBI) and opioid abuse have each reached epidemic proportions. An estimated 2.4 million Americans suffer a TBI each year[1], and in 2017 there were over 47,000 deaths due to opioid overdose[2]. The incidence of TBI among veterans of the military

has been approximated at 30%[3], with blast injury causing the overwhelming majority of TBIs in combat settings. Co-morbidity between non-severe TBI and substance abuse has been found in numerous civilian and military epidemiological studies[4–7], and there is evidence that opioid abuse may be particularly prevalent following TBI[8,9]. For example, in a study of >40,000 Air Force personnel, those that sustained mild TBI (compared to non-brain injuries) had elevated hazard ratios for several drugs of abuse[5]. Furthermore, the hazard ratio for opioids was higher than all other drugs of abuse in the 18 months following injury (including alcohol)[5].

MRI is a non-invasive technique that has been used to identify structural and functional consequences of TBI in humans and rodents. Experimental blast TBI has been shown to produce widespread decreases in fractional anisotropy (FA)[10], with closely-spaced repeated blast exposures exacerbating these effects[11]. Diffusion tensor imaging (DTI) measurements also tend to be exacerbated with time post-injury: we have reported an increase in the volume of microstructural damage between post-injury day 4 and 30[10], and Badea et al. have reported greater changes in DTI at 90 days relative to 7 days post-injury[12]. Changes in resting state functional connectivity (rsfc) have also been observed in human and experimental TBI. In veterans that sustained a mild TBI, increased intra-hemispheric connectivity of the anterior cingulate cortex was found in veterans that had experienced a mild TBI[13]. In collegiate athletes, elevated local connectivity (regional homogeneity: REHO) in the right middle and superior frontal gyri was associated with clinical symptoms following sports concussion[14]. Widespread disruptions in functional connectivity have also been associated with long-term effects of TBI (reviewed in[15–17]). In a study of high school and collegiate football players, increased widespread rsfc was observed only in athletes that remained symptomatic one week following injury[18]. Combat veterans that sustained blast mild TBI and had persistent post-concussive symptoms had increased rsfc (assessed by magnetoencephalography) in several brain regions, including the ventromedial cortex and anterior cingulate cortices[19].

Clinical studies have also identified structural and functional changes associated with opioid abuse. A voxel-based meta-analysis of studies on heroin users employing diffusion tensor imaging (DTI) found bilateral reductions in FA in frontal subgyral regions, including areas impacting the communication between cingulate and limbic association cortices with prefrontal association cortices[20]. Heroin dependent individuals were also found to have lower FA in the white matter tract connecting the mPFC and postcentral gyrus[21] and a comparison of heroin users that relapsed to those that remained abstinent 6 months after initiation of methadone maintenance therapy found lower FA in several white matter tracts in the relapse group[22]. In a neuroimaging study of over 150 subjects, increased widespread structural connectivity was reported in abstinent heroin users relative to non-heroin using controls[23]. In a study of former heroin users undergoing methadone maintenance, those that relapsed had elevated REHO in medial orbital cortex and the right caudate nucleus, and elevated REHO in the caudate was correlated with relapse rates[24]. In contrast, methadone maintained former heroin users had lower REHO in the medial orbital cortex compared to control subjects without a history of heroin or methadone use[25].

Despite extensive evidence of increased substance abuse disorder following TBI and high rates of opioid prescriptions to veterans and civilians that sustain TBI, little is known about how neurological damage associated with TBI may exacerbate opioid addiction liability and how opioid exposure may change TBI outcomes. The prefrontal cortex (PFC) and nucleus accumbens (NAc) are engaged during drug craving in human opioid users and drug seeking behaviors in rodent models of opioid addiction[26–28]. Substance use has been associated with structural and functional disruption of networks that include the PFC and NAc, such as executive and reward networks[20,21,29]. These brain regions[30–32] and networks[15,16,33] are also disrupted in blast and non-blast TBI, and this disruption has been posited as a mechanism by which TBI may increase susceptibility to risky substance use[34].

We have previously demonstrated that our blast model of mild TBI leads to enduring microstructural changes in the medial PFC[10] and that repeated blast mild TBI (rbTBI) persistently elevated levels of oxycodone seeking, despite similar levels of prior drug self-administration[35]. In this study, we used structural and functional MRI to examine the effects of TBI and oxycodone self-administration (SA) on changes in microstructure and functional connectivity. We hypothesized that rbTBI would disrupt these outcomes in the PFC, and that oxycodone SA would exacerbate the effects of rbTBI. We first tested this hypothesis by comparing group differences in principal components derived from all MRI measures from the PFC and NAc. We also tested the hypothesis that functional connectivity within the PFC and between the PFC and nucleus accumbens would be positively correlated with oxycodone seeking, based on the established role of the PFC and its efferents to the NAc in drug seeking (reviewed in[26,36]). Finally, we tested the hypothesis that rbTBI and oxycodone would disrupt widespread functional connectivity.

Materials and methods

An overview and timeline of experimental procedures is found in Fig 1A.

Animals

Male Sprague Dawley rats (Harlan/Envigo, Madison, WI, USA) arrived at the Zablocki Veterans Affairs Medical Center (ZVAMC) and were housed in pairs. Three days after the final blast or sham exposure, rats were transferred from the ZVAMC to Medical College of Wisconsin (MCW, approximately 5 miles away). Upon arrival at MCW, rats were singly housed for the remainder of the study. Food and water were provided ad libitum throughout the study, except when rats were in the behavioral apparatus. Animals were housed under a reverse light cycle (lights off 0730-1930), and experiments were conducted during the dark (awake) period. Experiments were conducted 5 days/week by experimenters blinded to the treatment condition. All experiments were conducted in compliance with the Institutional Animal Care and Use Committee (IACUC) at MCW and ZVAMC (protocol number: AUA 2816).

Repeated blast exposure

Rats were exposed to repeated blast overpressure or repeated sham conditions as described in[10,35,37,38]. During blast or sham treatment, rats were maintained under anesthesia with a

continuous delivery of 1.5% isoflurane and administered Rimadyl (carprofen, 5 mg/kg, s.c., Zoetis Inc, Kalamazoo, MI, USA). The torso of the rat was shielded with a metal cylinder, earplugs were inserted, and the head was restrained to prevent injury from rotational acceleration[10]. Blast-exposed rats were positioned 17 cm from the end of a custom shock tube (3.6 cm inner diameter, 3.0 m driven section and 0.3 m driver section with Mylar membrane between the driver and driven sections) and 18 deg off axis from the shock tube to prevent interaction of the head with exhaust gases. The animal was positioned so the head was orthogonal to the expanding shockwave, resulting in the left side of the head being exposed to the shockwave. Blast overpressure (450 kPa, 80 kPa*ms) was produced by pressurizing the driver section with helium until the membrane ruptured. Sham-exposed rats were subjected to the same procedures but were placed outside the overpressure shockwave. Following exposure, rats were placed on a heating pad and observed until return of righting reflex. Time from initiation of anesthesia prior to blast exposure until return of the righting reflex was quantified as 'recovery time'. Following recovery, rats were transferred back to their home cage, and periodically observed for 6 h. This procedure was conducted daily for 3 days as a repeated blast injury model. Sham-exposed rats received sham procedures daily for 3 days. Experimenters were blind to group assignment during subsequent phases of experiments.

Jugular catheterization surgery

Jugular catheterization was performed as described[35,39]. Rats were anesthetized with isoflurane (3–5% induction, 1–3% maintenance), and a silicone catheter (Silastic, ID: 0.51 mm, OD: 0.94 mm; Dow Corning, Auburn, MI, USA) was implanted into the right jugular vein and exited via the interscapular region. The catheter was connected to a cannula assembly: a 22-gauge stainless steel cannula (Plastics One, Roanoke, VA, USA) mounted on a base made from dental acrylic and nylon mesh, which was implanted subcutaneously. At the start of the surgery and the following day, Rimadyl (carprofen, 5 mg/kg, s.c. Zoetis Inc) was given. Catheters were flushed daily with 0.2 mL of heparinized saline (30 units/mL) and cefazolin (100 mg/mL). Rats recovered for at least 1 week prior to the start of the drug self-administration experiments.

Food training

Food training and oxycodone self-administration were performed as described in[35]. Food and oxycodone self-administration and the seeking test all took place in operant conditioning chambers (31.8 × 25.4 × 26.7 cm, Med Associates, Fairfax, VT, USA) which were enclosed in sound-attenuating boxes. Chambers were equipped with two retractable levers on either side of a central food receptacle on the right wall, cue lights above each lever and a house light located on the left wall near the ceiling. Computer-controlled infusion pumps held syringes that were connected to tubing and liquid swivels. Sound attenuating boxes had a software-controlled exhaust fan.

Rats began by learning to self-administer food (fruit punch flavored 45 mg sucrose tablets, LabDiet, St. Louis, MO, USA) without food restriction. Each session lasted for 2 h/day unless the maximum number of rewards (64 sucrose pellets) was met prior to the conclusion of the 2 h. At the beginning of each session, the fan was turned on, both levers were

extended, and a sucrose pellet was delivered. Rats were first trained on a fixed ratio (FR)-1 schedule of reinforcement, with a single press on the active lever resulting in sucrose pellet delivery. After meeting criteria (three consecutive days with ≥ 50 rewards earned and ≥ 70% of total lever presses on the active lever, 4 day minimum), rats performed a single food self-administration session on an FR-2 schedule of reinforcement (2 active lever presses required per reward).

The active lever was assigned to be on either the left or right side, and lever assignment was counterbalanced between rats within each group. After reward delivery, a 10 s timeout began, and the cue light above the active lever was illuminated for 5 s. During the timeout period, active and inactive lever responses were recorded but had no programmed consequence. Throughout the entire session, responses on the inactive lever were recorded but also had no programmed consequence.

Oxycodone self-administration and seeking

After completion of food training, rats in the rbTBI and sham groups were further divided into those that self-administered oxycodone (0.1 mg/kg/infusion) or received yoked infusions of saline. The oxycodone dose was chosen based on prior self-administration studies in the rat and to replicate our prior work[35,40,41]. Each yoked saline rat was matched to a “master” rat from the same cohort. When the “master” rat earned an infusion of oxycodone, the yoked rat received an infusion of saline at the exact same time (computer controlled). Thus, the infusion history between the “master” and “yoke” rats is identical, controlling for the potential influence of infusions. Yoked saline rats still received cue light presentation in response to completing the response requirements. The infusion volume and time varied for each rat to ensure the appropriate dose was delivered from the stock solution (e.g., a 300 g rat received a 40 μL infusion over 1.6 s) and yoked saline rats received weight-corrected volumes of saline. This phase consisted of 10 daily 2-h sessions (maximum 96 infusions/session): 5 d each on FR-2 and FR-4 schedules of reinforcement. Catheter patency was determined after completion of the self-administration sessions using Brevital (methohexital, 9 mg/kg, i.v.; JHP Pharmaceuticals, Rochester, MI, USA) and any rat that did not meet criteria for patency (sedation within 10 s) was removed from the study. Three days after completion of the 10-day oxycodone self-administration (or yoked saline) phase, all rats were placed back into the operant conditioning chambers for a drug seeking test under extinction conditions. Completion of the FR-4 schedule resulted in saline infusion and cue delivery for all animals (i.e., yoked saline animals were no longer yoked).

Magnetic Resonance Imaging (MRI)

In vivo magnetic resonance imaging was performed on a Bruker 9.4 T Biospec System. A Bruker Biospin 4-channel surface coil array was used for signal reception and transmission was achieved via a 72 mm diameter quadrature volume coil. Heart rate (ECG), core temperature, and respiration were monitored continuously. Anesthesia was induced with isoflurane (3.0%), which was tapered to 0% after initiation of constant tail vain infusion of dexmedetomidine. Dexmedetomidine was chosen for anesthesia maintenance due to the reduced impact on the BOLD signal compared to isoflurane[42]. Dexmedetomidine was delivered via constant tail vain infusion (initial concentration: 50 μg/kg/hr) and was titrated

to maintain anesthetic depth as determined by ECG, body temperature, and respiratory rate. Anesthetized rats were secured to a custom-made temperature-controlled cradle to minimize motion. A high-resolution anatomical image was acquired with an isotropic resolution of 134 μm^3. For diffusion imaging, a 4-shot spin-echo echo planar imaging (DW-EPI) sequence was used as described previously[43] with TR=2000 and TE=23 ms, including fat saturation using both chemical shift-selective saturation and gradient reversal of the refocusing pulse slice. Thirty slices covered the entire brain at an in-plane resolution of 0.30×0.30 mm^2, slice thickness of 0.8 mm and 0.3 mm slice gap. Two signal averages were used to acquire 60 unique diffusion directions[44] at each b-value of 250, 1000, and 2000 s/mm^2 with 8 non-diffusion-weighted images. For resting state functional MRI, 200 images were acquired at a temporal resolution of 3 sec using single-shot gradient echo EPI at the identical spatial resolution. Three images were acquired for each repetition at echo times of 16.5, 33.1, and 49.6 ms, and each run was repeated 3 times for a total of 30 minutes for fMRI data acquisition. To examine for any evidence of overt injury or hemorrhage, a 3D multiple echo acquisition with 0.175 mm^3 isotropic voxels (TR=50 ms) was acquired with 10 echo times between 2.2 and 24.9 ms. Across all animals, no hemorrhage was evident based on visual inspection.

Images were processed using the Analysis of Functional Neuroimages (AFNI; Bathesda, MD) and the FMRIB Software Library (FSL, University of Oxford) software packages. Preprocessing of fMRI included multi-echo combination[45], slice-timing correction, motion correction, and bandpass filtering between 0.01 and 0.1 Hz. Diffusion weighted images were corrected for motion and the diffusion tensor was computed to generate maps of fractional anisotropy (FA), and mean diffusivity (MD) using the FMRI Software Library (FSL). fMRI timeseries and DTI maps were spatially registered to a rat MRI brain template[46] using the T_2-weighted anatomical images as an intermediate step to align the mean fMRI and non-diffusion weighted images. Regions of interest (ROIs) were defined in template space using an aligned Paxinos and Watson atlas for anatomical delineation, which focused on the prelimbic prefrontal cortex (PrL), infralimbic prefrontal cortex (IL), nucleus accumbens (NAc), and orbitofrontal cortex (OFC) using separate left and right regions. Connectivity between these ROIs was calculated as the temporal Pearson correlation coefficient in the BOLD timeseries between pairwise regions. An fMRI measure of the regional heterogeneity (REHO) and DTI measures of fractional anisotropy and mean diffusivity were derived as the mean values within each ROI.

Statistical Analysis

Statistical tests were performed using Prism 8 (GraphPad, San Diego, CA, USA) or SPSS Statistics 24 (IBM, Inc.) software. Data were analyzed using mixed model ANOVAs with Holm-Sidak post hoc tests. ANOVAs were performed using ranked data if data did not fit a normal distribution as determined by D'Agonstino & Pearson tests. Correlational analyses were performed using linear regressions (Spearman rank correlations if data did not fit a normal distribution). Differences were considered significant when $p \leq 0.05$. Principal components analysis was performed using oblique rotation (direct oblim method in SPSS) and components that explained ≥ 5% variance were retained.

Results

Behavioral measures

Acquisition of operant conditioning—On week three following rbTBI or sham treatment, rats underwent food self-administration training. Food self-administration did not differ between rats exposed to rbTBI and sham (main and interaction effects of rbTBI all $\eta^2<0.045$, $p>0.39$; Fig 1B). These data indicate that there was no impact of injury on the ability to acquire and perform this task, a critical consideration in TBI research that utilizes operant conditioning[47].

Self-administration—There was no significant difference between rbTBI and sham rats in oxycodone self-administration as measured by active lever presses during each FR phase (main and interaction effects of rbTBI all $\eta^2<0.065$, $p>0.21$; Fig 2A) or number of infusions earned during the FR-2 phase (main and interaction effects of rbTBI both $\eta^2<0.045$, $p>0.26$; Fig 2C) or the FR-4 phase (main and interaction effects of rbTBI all $\eta^2<0.083$, $p>0.16$; Fig 2D). There was also no significant difference in lever pressing between rbTBI and sham rats in the yoked saline groups (main and interaction effects of rbTBI both $\eta^2<0.016$, $p>0.67$; Fig 2B).

Oxycodone seeking—As expected, there was a significant effect of drug on oxycodone seeking ($F(1, 40)=53.28$, $\eta^2=0.55$, $p<0.0001$), but there was no effect of injury or interaction (both $\eta^2<0.026$, $p>0.12$). Since we had previously demonstrated a TBI-associated increase in drug seeking using the same TBI and oxycodone self-administration procedures[35], we performed a planned comparison on oxycodone seeking between sham and rbTBI animals. Compared to sham injured rats, rbTBI rats had greater drug seeking during testing under extinction conditions (no drug available) ($t(10)=2.38$, $d=0.72$, $p=0.039$; Fig 2E).

MRI

To examine neuroimaging correlates of injury and oxycodone self-administration, rats underwent structural and functional MRI at 7-weeks post-injury, approximately 10 days following cessation of oxycodone self-administration.

Principal Components Analysis (PCA)—Data were first analyzed using principal components analysis to reduce the dimensionality of total MRI dataset. PCA identified four components that explained a total of 73.9% of the variance (Fig 3A). Principal component 1 (PC1) had strong loading from all functional connectivity measures, including REHO (Fig 3B). PC2 reflected microstructural outcomes, having strong inverse loading from FA and positive loading from MD. PC3 was primarily loaded by local connectivity (REHO), while PC4 had loadings from FA and to a lesser extent rsfc. PC4 also had distinct loadings from the ipsilateral and contralateral sides of the PrL and IL. Plotting experimental groups on PC1 and PC2 showed distinct patterns of separation for rbTBI and oxycodone SA groups. Oxycodone SA groups differed more from sham/saline in PC1, whereas injury was more associated with differences in PC2. Plotting PC1 and PC3 resulted in isolation of the sham/oxySA group from a cluster of the remaining groups, including the rbTBI/oxySA group. Principal component correlations showed that PC3 and PC4 had the greatest

associations with oxycodone seeking, especially in rbTBI rats (Fig 3F). Correlations with oxycodone intake showed similar trends, with PC2 also showing inverse associations that were consistent between sham and rbTBI rats (Fig 3G).

Structural MRI—Structural assessment was performed by examining T2, T2*3D, fractional anisotropy (FA), and mean diffusivity (MD). We examined main and interactive effects of rbTBI and oxycodone self-administration on microstructure of the prefrontal cortex and nucleus accumbens. There were no significant main effects of injury or oxycodone on FA or MD in the PFC or NAc, but a significant TBI x oxycodone interaction was found in the FA of both hemispheres of the NAc ($p \leq 0.05$).

Structural MRI: Relationship to oxycodone seeking—We have previously demonstrated that bTBI lead to changes in hippocampal FA that correlated with spatial learning deficits[10]. To examine the possibility that mPFC FA was associated with drug seeking, we performed correlational analyses between FA in the subregions of the prefrontal cortex (PFC) and nucleus accumbens (NAc) and active lever presses during the drug seeking session. We examined sham and rbTBI rats separately and together to determine if associations were specific to injured rats or if associations generalized to both populations. Within the PFC, inverse associations were primarily limited to the PrL and IL ipsilateral to injury and were present in all experimental groups ($r = -0.34$ to -0.64; Fig 4A). The NAc also showed inverse correlations between FA and oxycodone seeking, but this effect was primarily in rbTBI rats ($r = -0.42$ to -0.46). Examination of MD found associations between some of the regions and drug seeking, but these effects were largely isolated to the sham injured rats (Fig 4B).

Structural MRI: Relationship to oxycodone intake during self-administration—To determine if the associations with drug seeking were explained by the amount of oxycodone intake during prior self-administration sessions, we examined the correlations between the microstructural measures and drug intake. There was a pattern of negative associations between FA and drug intake in ipsilateral PrL and IL that was similar to those observed with drug seeking, although the effects were smaller for intake (Fig 4C). There was also a positive linear association between the FA and prior oxycodone intake in the contralateral IL that was most pronounced in the rbTBI and sham+rbTBI rats (rho= 0.39 to 0.65; Fig 4C). The MD in both hemispheres of the OFC had strong positive associations with oxycodone intake in sham rats (rho= - −0.46 to −0.73), while the IL had robust negative associations with intake in rbTBI rats (rho= −0.67 for each hemisphere; Fig 4D). There were also strong positive associations between MD and oxycodone intake in the OFC of sham animals (rho=0.73 and 0.46 in ipsilateral and contralateral hemispheres, respectively)

Functional MRI—Next, two types of functional MRI analyses were performed: resting state regional homogeneity (REHO, a voxelwise measure of local connectivity) and functional connectivity (rsfc), a measure of connectivity between brain regions. REHO found very few effects of rbTBI or oxycodone self-administration alone, but significant interaction effects were identified in prefrontal cortex, nucleus accumbens, and several other regions (Fig 5). In rsfc, rbTBI/saline and sham/oxycodone self-administration rats

showed comparable patterns of connectivity to sham/saline rats, while rbTBI/oxycodone self-administration rats had a larger number of connected nodes, as defined by Pearson r≥0.6 (Fig 6). Edge strengths were tested in a factorial design, which also yielded a significant interaction ($p \leq 0.05$), but no significant main effects (both $p > 0.62$).

Functional MRI: Relationship to oxycodone seeking and intake—Pairwise correlations were performed on each hemisphere of the OFC, PrL, IL, and NAc (Fig 7). Analysis of the relationship between functional connectivity and drug seeking (active lever presses during extinction session) found that the inter-hemispheric connectivity of the OFC and IL were positively correlated with drug seeking in injured rats and uninjured rats (Fig 7C). Prefrontal-accumbens functional connectivity was highly associated with drug intake on the left hemisphere (ipsilateral to injury in rbTBI rats), and this was observed in rbTBI and the combined population of rats (rho= 0.66 and 0.56, respectively; Fig 7E,F).

Discussion

We have previously shown that rbTBI-exposed rats had elevated drug seeking following oxycodone self-administration despite similar levels of drug intake[35]. We replicated this finding and also demonstrated that rbTBI does not lead to generalized deficits in extinction learning (i.e., extinction of sucrose pellet seeking). This is an important finding considering that we have previously reported that rbTBI resulted in elevated oxycodone seeking in extinction conditions[35] and several studies have found that mild TBI impaired extinction of conditioned fear[48–50]. rbTBI may have promoted incubation of drug craving[51,52], and the lack of rbTBI-associated change in sucrose extinction supports this mechanism over a generalized extinction deficit. Ongoing experiments are testing for incubation of opioid craving in a timecourse series.

In this study, we used neuroimaging to explore potential interactive effects and correlates of behavior on structural and functional brain networks. PCA identified components representing functional connectivity (PC1), microstructure (PC2), and local connectivity (PC3) as contributing the most to the overall variance in the MRI data from frontal cortical regions and the NAc. The component representing functional connectivity (PC1) was impacted more by oxycodone SA, while the microstructure component (PC2) was more impacted by injury. Like PC1, PC3 was also impacted by oxycodone, which differed in rats with rbTBI. The nature of these interaction is somewhat different than the interaction observed in voxelwise REHO analyses, which indicated subthreshold main effects of rbTBI or injury. We found several neuroimaging metrics that were associated with drug seeking behavior, prior drug intake, and interactive effects of injury and oxycodone self-administration. Microstructural analysis identified negative associations between FA and drug seeking in the left (but not right) PrL and IL PFC, the side ipsilateral to injury in rbTBI rats. The effect was largest in rbTBI rats but was also present in the combined population of injured and un-injured rats. The associations between FA and seeking were greater than FA and drug intake, suggesting that the effects were not entirely explained by the amount of oxycodone self-administered. Within the NAc, there was a significant interaction between injury and oxycodone self-administration on FA, and this was accompanied by inverse relationships between FA and seeking and between MD and oxycodone intake.

The correlations between FA and drug seeking had larger effects in injured relative to uninjured rats, suggesting that rbTBI enabled or enhanced the emergence of a relationship between this structural parameter of the PFC and prior drug seeking. Resting state functional connectivity (rsfc) analyses found a widespread increase in network connectivity only in rats that received both injury and oxycodone SA. There were also positive correlations between inter-hemispheric connectivity and drug seeking in the OFC and IL, and between ipsilateral IL – NAc connectivity and oxycodone intake during self-administration. As observed in the structural measures, the OFC and IL – NAc effects were largest in injured animals, suggesting the interaction of injury and oxycodone exposure enabled the emergence of a relationship between functional connectivity and prior drug seeking and/or drug intake. An interaction was also measured in local connectivity: regional homogeneity was minimally affected by injury or oxycodone self-administration alone, but animals receiving both had marked increases in voxelwise homogeneity of the medial PFC, NAc, and several other areas. Comparison of data from PCA to correlations from individual outcome measures and brain regions yielded distinct but complementary results. Components 1–3 primarily represented either structural or functional MRI measures with minor differences in loadings between different brain regions. Component 4 primarily represented structural outcomes from prefrontal regions that were lateralized. Components 3 and 4 showed the highest associations with oxycodone seeking and intake, with similar effect sizes as the strongest correlations from individual regions. Comparison of these data also highlighted the IL as a key brain region that associates with oxycodone intake and seeking, especially in inured rats. This was evident in its contributions to PC4, as well as correlations with intake and seeking in structural and functional MRI outcomes.

The significance of injury and opioid exposure has been examined in peripheral and central injury models. Mu opioid receptor agonists administered after injury lead to longer recovery times in models of spinal cord injury and neuropathic pain[53–55]. Regarding TBI, the impact of opioid exposure on injury outcomes is less clear. Fentanyl administered immediately following controlled cortical impact exacerbated motor and spatial learning deficits within three weeks of injury[56]. In a comparison of multiple anesthetic agents delivered immediately after controlled cortical impact, morphine was associated with the worst outcomes on motor performance in the first five days after injury, while fentanyl was associated with the worst performance in the Morris water maze two weeks following injury[57]. In the present study, we observed several interactive effects between rbTBI and oxycodone self-administration consistent with worse outcomes (outlined in the above section).

Neuroimaging studies of TBI

Prior studies using DTI have identified microstructural damage following TBI[10–12]. We did not see altered FA or MD after TBI or oxycodone SA alone, but there was an interaction of injury and drug on FA in the NAc. Prior studies have also identified changes in resting state functional connectivity. For example, regions of the PFC had increased inra- and inter-hemispheric connectivity in collegiate athletes that had experienced a mild TBI[13,58], an effect we observed in the PrL and IL (immediately ventral of the anterior cingulate cortex in the rat). We also found increased widespread and local connectivity in injured rats that self-administered oxycodone, but not in rats that only received injury or opioid. Similar to

our observation of increased inter-hemispheric connectivity within the OFC and IL, Kulkarni et al. reported increased rsfc within PrL and IL after a single closed head momentum exchange injury[59].

Neuroimaging studies of opioid use

In the present study, we found that rats receiving rbTBI and oxycodone self-administration had elevated REHO in several prefrontal regions, including medial and lateral orbital cortex. Local connectivity has not been extensively studied after opioid exposure, but REHO was found to be lower in the PFC of former heroin users that were maintained on methadone[25]. Differences between our data and[25] may arise from the interactive effects of the oxycodone and injury, the lack of opioid maintenance therapy in our rodent study, or other experimental differences. In regard to rsfc, Zhou et al. found increased functional connectivity between the ventromedial PFC and nucleus accumbens in former heroin users with >= 3 years of abstinence[60], similar to our findings of increased functional connectivity between ventral/rostral anterior cingulate cortex and the nucleus accumbens[61]. Increased widespread functional connectivity has also been reported in heroin use during abstinence[62] and in rodent models of withdrawal from alcohol, nicotine, cocaine, or methamphetamine[63,64]. There are also findings of decreased rsfc in opioid addiction, especially when examining connectivity within an executive network (reviewed in[65,66]). These conflicting results may be due to differences in abstinence time and/or opioid maintenance therapy. We observed several instances of lateralized associations of functional connectivity with drug seeking, especially in the ipsilateral IL. This may be due to the drug, injury, or both. Few studies have addressed lateralization of drug effects on functional connectivity in rodents, but one study found that developmental exposure to alcohol reduced functional connectivity PFC connectivity with the left, but not right hemisphere of rats in adulthood[67]. Similarly, ethanol withdrawal asymmetrically altered neurochemistry in the PFC[68], and levels of dopamine metabolites in the right, but not left PFC correlated with future morphine self-administration[69]. In regard to our results from rbTBI rats, we have previously reported that our single blast TBI model produces microstructural changes that are unilateral 4 days following injury, but the injury becomes bilateral by 30 days post-injury[10]. The use of repeated blast TBI and oxycodone self-administration, or the longer duration between injury and neuroimaging (7 weeks vs. 4 weeks) in the present study may explain the enduring lateralization observed here.

Conclusions

In conclusion, we find evidence that repeated mild TBI and oxycodone interact in such a way that manifests as elevated drug seeking, increased microstructural damage, and widespread aberrant functional connectivity. This pattern of findings suggest that opioid exposure exacerbates the effects of TBI and results in increased drug seeking after abstinence. Our findings focused on a single timepoint of opioid exposure and drug seeking after injury. Future studies are needed to determine if this effect is observed with different times between injury and opioid exposure and if the interactive effects of TBI and opioids persist for a longer period of time.

Supplementary Material

Refer to Web version on PubMed Central for supplementary material.

Acknowledgements

This material is based upon work supported (or supported in part) by the Department of Veterans Affairs, Veterans Health Administration, Office of Research and Development (RX002931). This research was also supported by National Institute on Drug Abuse Grant DA039276 and the Research and Education Initiative Fund, a component of the Advancing a Healthier Wisconsin Endowment at the Medical College of Wisconsin. The content is solely the responsibility of the authors and does not necessarily represent the official views of the National Institutes of Health.

References

1. Taylor CA, Bell JM, Breiding MJ, Xu L. Traumatic Brain Injury-Related Emergency Department Visits, Hospitalizations, and Deaths - United States, 2007 and 2013. MMWR Surveill Summ. 2017;66(9):1–16.
2. Scholl L, Seth P, Kariisa M, Wilson N, Baldwin G. Drug and Opioid-Involved Overdose Deaths — United States, 2013–2017. MMWR Morb Mortal Wkly Rep. 2019;67:1419–1427.
3. Tanielian T, Jaycox LH, eds. Invisible wounds of war: Psychological and cognitive injuries, their consequences, and services to assist recovery. Rand Corportation; 2008; No. MG-720-CCF.
4. Fann JR, Burington B, Leonetti A, Jaffe K, Katon WJ, Thompson RS. Psychiatric illness following traumatic brain injury in an adult health maintenance organization population. Arch Gen Psychiatry. 2004;61(1):53–61. [PubMed: 14706944]
5. Miller SC, Baktash SH, Webb TS, et al. Risk for addiction-related disorders following mild traumatic brain injury in a large cohort of active-duty U.S. airmen. Am J Psychiatry. 2013;170(4):383–390. [PubMed: 23429886]
6. Corrigan JD. Substance abuse as a mediating factor in outcome from traumatic brain injury. Arch Phys Med Rehabil. 1995;76(4):302–309. [PubMed: 7717829]
7. Bjork JM, Grant SJ. Does traumatic brain injury increase risk for substance abuse? J Neurotrauma. 2009;26(7):1077–1082. [PubMed: 19203230]
8. Adams RS, Corrigan JD, Dams-O'Connor K. Opioid Use among Individuals with Traumatic Brain Injury: A Perfect Storm? J Neurotrauma. 2019.
9. Corrigan JD, Adams RS. The intersection of lifetime history of traumatic brain injury and the opioid epidemic. Addict Behav. 2019;90:143–145. [PubMed: 30391775]
10. Budde MD, Shah A, McCrea M, Cullinan WE, Pintar FA, Stemper BD. Primary blast traumatic brain injury in the rat: relating diffusion tensor imaging and behavior. Front Neurol. 2013;4:154. [PubMed: 24133481]
11. Calabrese E, Du F, Garman RH, et al. Diffusion tensor imaging reveals white matter injury in a rat model of repetitive blast-induced traumatic brain injury. J Neurotrauma. 2014;31(10):938–950. [PubMed: 24392843]
12. Badea A, Kamnaksh A, Anderson RJ, Calabrese E, Long JB, Agoston DV. Repeated mild blast exposure in young adult rats results in dynamic and persistent microstructural changes in the brain. Neuroimage Clin. 2018;18:60–73. [PubMed: 29868442]
13. Sheth C, Rogowska J, Legarreta M, McGlade E, Yurgelun-Todd D. Functional connectivity of the anterior cingulate cortex in Veterans with mild traumatic brain injury. Behav Brain Res. 2021;396:112882. [PubMed: 32853657]
14. Meier TB, Giraldo-Chica M, Espana LY, et al. Resting-State fMRI Metrics in Acute Sport-Related Concussion and Their Association with Clinical Recovery: A Study from the NCAA-DOD CARE Consortium. J Neurotrauma. 2020;37(1):152–162. [PubMed: 31407610]
15. Caeyenberghs K, Verhelst H, Clemente A, Wilson PH. Mapping the functional connectome in traumatic brain injury: What can graph metrics tell us? Neuroimage. 2017;160:113–123. [PubMed: 27919750]

16. Hayes JP, Bigler ED, Verfaellie M. Traumatic Brain Injury as a Disorder of Brain Connectivity. J Int Neuropsychol Soc. 2016;22(2):120–137. [PubMed: 26888612]
17. Sharp DJ, Scott G, Leech R. Network dysfunction after traumatic brain injury. Nat Rev Neurol. 2014;10(3):156–166. [PubMed: 24514870]
18. Kaushal M, Espana LY, Nencka AS, et al. Resting-state functional connectivity after concussion is associated with clinical recovery. Hum Brain Mapp. 2019;40(4):1211–1220. [PubMed: 30451340]
19. Huang MX, Harrington DL, Robb Swan A, et al. Resting-State Magnetoencephalography Reveals Different Patterns of Aberrant Functional Connectivity in Combat-Related Mild Traumatic Brain Injury. J Neurotrauma. 2017;34(7):1412–1426. [PubMed: 27762653]
20. Wollman SC, Alhassoon OM, Stern MJ, et al. White matter abnormalities in long-term heroin users: a preliminary neuroimaging meta-analysis. Am J Drug Alcohol Abuse. 2015;41(2):133–138. [PubMed: 25664621]
21. Ma X, Qiu Y, Tian J, et al. Aberrant default-mode functional and structural connectivity in heroin-dependent individuals. PLoS One. 2015;10(4):e0120861. [PubMed: 25859661]
22. Li W, Zhu J, Li Q, et al. Brain white matter integrity in heroin addicts during methadone maintenance treatment is related to relapse propensity. Brain Behav. 2016;6(2):e00436. [PubMed: 27110449]
23. Sun Y, Wang GB, Lin QX, et al. Disrupted white matter structural connectivity in heroin abusers. Addict Biol. 2017;22(1):184–195. [PubMed: 26177615]
24. Chang H, Li W, Li Q, et al. Regional homogeneity changes between heroin relapse and non-relapse patients under methadone maintenance treatment: a resting-state fMRI study. BMC Neurol. 2016;16(1):145. [PubMed: 27538517]
25. Qiu YW, Han LJ, Lv XF, et al. Regional homogeneity changes in heroin-dependent individuals: resting-state functional MR imaging study. Radiology. 2011;261(2):551–559. [PubMed: 21875854]
26. Reiner DJ, Fredriksson I, Lofaro OM, Bossert JM, Shaham Y. Relapse to opioid seeking in rat models: behavior, pharmacology and circuits. Neuropsychopharmacology. 2019;44(3):465–477. [PubMed: 30293087]
27. Langleben DD, Ruparel K, Elman I, et al. Extended-release naltrexone modulates brain response to drug cues in abstinent heroin-dependent patients. Addict Biol. 2014;19(2):262–271. [PubMed: 22747521]
28. Li Q, Li W, Wang H, et al. Predicting subsequent relapse by drug-related cue-induced brain activation in heroin addiction: an event-related functional magnetic resonance imaging study. Addict Biol. 2015;20(5):968–978. [PubMed: 25214465]
29. Zilverstand A, Huang AS, Alia-Klein N, Goldstein RZ. Neuroimaging Impaired Response Inhibition and Salience Attribution in Human Drug Addiction: A Systematic Review. Neuron. 2018;98(5):886–903. [PubMed: 29879391]
30. Taylor PA, Ford CC. Simulation of blast-induced early-time intracranial wave physics leading to traumatic brain injury. J Biomech Eng. 2009;131(6):061007. [PubMed: 19449961]
31. Mu W, Catenaccio E, Lipton ML. Neuroimaging in Blast-Related Mild Traumatic Brain Injury. J Head Trauma Rehabil. 2017;32(1):55–69. [PubMed: 27022955]
32. Eierud C, Craddock RC, Fletcher S, et al. Neuroimaging after mild traumatic brain injury: review and meta-analysis. Neuroimage Clin. 2014;4:283–294. [PubMed: 25061565]
33. Wolf JA, Koch PF. Disruption of Network Synchrony and Cognitive Dysfunction After Traumatic Brain Injury. Front Syst Neurosci. 2016;10:43. [PubMed: 27242454]
34. Olsen CM, Corrigan JD. Does Traumatic Brain Injury Cause Risky Substance Use or Substance Use Disorder? Biol Psychiatry. 2021.
35. Nawarawong NN, Slaker M, Muelbl M, et al. Repeated blast model of mild traumatic brain injury alters oxycodone self-administration and drug seeking. Eur J Neurosci. 2019;50(3):2101–2112. [PubMed: 30456793]
36. Kalivas PW, Volkow ND. The neural basis of addiction: a pathology of motivation and choice. Am J Psychiatry. 2005;162(8):1403–1413. [PubMed: 16055761]

37. Lim YW, Meyer NP, Shah AS, Budde MD, Stemper BD, Olsen CM. Voluntary Alcohol Intake following Blast Exposure in a Rat Model of Mild Traumatic Brain Injury. PLoS One. 2015;10(4):e0125130. [PubMed: 25910266]
38. Stemper BD, Shah AS, Budde MD, et al. Behavioral Outcomes Differ between Rotational Acceleration and Blast Mechanisms of Mild Traumatic Brain Injury. Frontiers in Neurology. 2016;7(31).
39. Muelbl MJ, Slaker ML, Shah AS, et al. Effects of Mild Blast Traumatic Brain Injury on Cognitive- and Addiction-Related Behaviors. Sci Rep. 2018;8(1):9941. [PubMed: 29967344]
40. Mavrikaki M, Pravetoni M, Page S, Potter D, Chartoff E. Oxycodone self-administration in male and female rats. Psychopharmacology (Berl). 2017;234(6):977–987. [PubMed: 28127624]
41. Blackwood CA, Leary M, Salisbury A, McCoy MT, Cadet JL. Escalated Oxycodone Self-Administration Causes Differential Striatal mRNA Expression of FGFs and IEGs Following Abstinence-Associated Incubation of Oxycodone Craving. Neuroscience. 2019;415:173–183. [PubMed: 31351142]
42. Pawela CP, Hudetz AG, Ward BD, et al. Modeling of region-specific fMRI BOLD neurovascular response functions in rat brain reveals residual differences that correlate with the differences in regional evoked potentials. Neuroimage. 2008;41(2):525–534. [PubMed: 18406628]
43. Skinner NP, Kurpad SN, Schmit BD, Tugan Muftuler L, Budde MD. Rapid in vivo detection of rat spinal cord injury with double-diffusion-encoded magnetic resonance spectroscopy. Magn Reson Med. 2017;77(4):1639–1649. [PubMed: 27080726]
44. Basser PJ, Mattiello J, LeBihan D. Estimation of the effective self-diffusion tensor from the NMR spin echo. J Magn Reson B. 1994;103(3):247–254. [PubMed: 8019776]
45. Kundu P, Inati SJ, Evans JW, Luh WM, Bandettini PA. Differentiating BOLD and non-BOLD signals in fMRI time series using multi-echo EPI. Neuroimage. 2012;60(3):1759–1770. [PubMed: 22209809]
46. Valdes-Hernandez PA, Sumiyoshi A, Nonaka H, et al. An in vivo MRI Template Set for Morphometry, Tissue Segmentation, and fMRI Localization in Rats. Front Neuroinform. 2011;5:26. [PubMed: 22275894]
47. Vonder Haar C, Winstanley CA. Minor Functional Deficits in Basic Response Patterns for Reinforcement after Frontal Traumatic Brain Injury in Rats. J Neurotrauma. 2016;33(20):1892–1900. [PubMed: 26756392]
48. Schneider BL, Ghoddoussi F, Charlton JL, et al. Increased Cortical Gamma-Aminobutyric Acid Precedes Incomplete Extinction of Conditioned Fear and Increased Hippocampal Excitatory Tone in a Mouse Model of Mild Traumatic Brain Injury. J Neurotrauma. 2016;33(17):1614–1624. [PubMed: 26529240]
49. Zhao J, Huynh J, Hylin MJ, et al. Mild Traumatic Brain Injury Reduces Spine Density of Projection Neurons in the Medial Prefrontal Cortex and Impairs Extinction of Contextual Fear Memory. J Neurotrauma. 2018;35(1):149–156. [PubMed: 28665166]
50. Cheng WH, Martens KM, Bashir A, et al. CHIMERA repetitive mild traumatic brain injury induces chronic behavioural and neuropathological phenotypes in wild-type and APP/PS1 mice. Alzheimers Res Ther. 2019;11(1):6. [PubMed: 30636629]
51. Grimm JW, Hope BT, Wise RA, Shaham Y. Neuroadaptation. Incubation of cocaine craving after withdrawal. Nature. 2001;412(6843):141–142. [PubMed: 11449260]
52. Theberge FR, Pickens CL, Goldart E, et al. Association of time-dependent changes in mu opioid receptor mRNA, but not BDNF, TrkB, or MeCP2 mRNA and protein expression in the rat nucleus accumbens with incubation of heroin craving. Psychopharmacology (Berl). 2012;224(4):559–571. [PubMed: 22790874]
53. Grace PM, Strand KA, Galer EL, et al. Morphine paradoxically prolongs neuropathic pain in rats by amplifying spinal NLRP3 inflammasome activation. Proc Natl Acad Sci U S A. 2016;113(24):E3441–3450. [PubMed: 27247388]
54. Gaudet AD, Ayala MT, Schleicher WE, et al. Exploring acute-to-chronic neuropathic pain in rats after contusion spinal cord injury. Exp Neurol. 2017;295:46–54. [PubMed: 28552717]

55. Loram LC, Grace PM, Strand KA, et al. Prior exposure to repeated morphine potentiates mechanical allodynia induced by peripheral inflammation and neuropathy. Brain Behav Immun. 2012;26(8):1256–1264. [PubMed: 22902523]
56. Statler KD, Kochanek PM, Dixon CE, et al. Isoflurane improves long-term neurologic outcome versus fentanyl after traumatic brain injury in rats. J Neurotrauma. 2000;17(12):1179–1189. [PubMed: 11186231]
57. Statler KD, Alexander H, Vagni V, et al. Comparison of seven anesthetic agents on outcome after experimental traumatic brain injury in adult, male rats. J Neurotrauma. 2006;23(1):97–108. [PubMed: 16430376]
58. Czerniak SM, Sikoglu EM, Liso Navarro AA, et al. A resting state functional magnetic resonance imaging study of concussion in collegiate athletes. Brain Imaging Behav. 2015;9(2):323–332. [PubMed: 25112544]
59. Kulkarni P, Morrison TR, Cai X, et al. Neuroradiological Changes Following Single or Repetitive Mild TBI. Front Syst Neurosci. 2019;13:34. [PubMed: 31427931]
60. Zou F, Wu X, Zhai T, et al. Abnormal resting-state functional connectivity of the nucleus accumbens in multi-year abstinent heroin addicts. J Neurosci Res. 2015;93(11):1693–1702. [PubMed: 26280556]
61. Ma N, Liu Y, Li N, et al. Addiction related alteration in resting-state brain connectivity. Neuroimage. 2010;49(1):738–744. [PubMed: 19703568]
62. Liu J, Liang J, Qin W, et al. Dysfunctional connectivity patterns in chronic heroin users: an fMRI study. Neurosci Lett. 2009;460(1):72–77. [PubMed: 19450664]
63. Kimbrough A, Lurie DJ, Collazo A, et al. Brain-wide functional architecture remodeling by alcohol dependence and abstinence. Proc Natl Acad Sci U S A. 2020;117(4):2149–2159. [PubMed: 31937658]
64. Kimbrough A, Kallupi M, Smith LC, Simpson S, Collazo A, George O. Characterization of the brain functional architecture of psychostimulant withdrawal using single-cell whole brain imaging. eneuro. 2021:ENEURO.0208–0219.2021.
65. Pandria N, Kovatsi L, Vivas AB, Bamidis PD. Resting-state Abnormalities in Heroin-dependent Individuals. Neuroscience. 2018;378:113–145. [PubMed: 27884551]
66. Ieong HF, Yuan Z. Resting-State Neuroimaging and Neuropsychological Findings in Opioid Use Disorder during Abstinence: A Review. Front Hum Neurosci. 2017;11:169. [PubMed: 28428748]
67. Tang S, Xu S, Waddell J, Zhu W, Gullapalli RP, Mooney SM. Functional Connectivity and Metabolic Alterations in Medial Prefrontal Cortex in a Rat Model of Fetal Alcohol Spectrum Disorder: A Resting-State Functional Magnetic Resonance Imaging and in vivo Proton Magnetic Resonance Spectroscopy Study. Dev Neurosci. 2019;41(1–2):67–78. [PubMed: 30999297]
68. Carlson JN, Drew Stevens K. Individual differences in ethanol self-administration following withdrawal are associated with asymmetric changes in dopamine and serotonin in the medial prefrontal cortex and amygdala. Alcohol Clin Exp Res. 2006;30(10):1678–1692. [PubMed: 17010135]
69. Glick SD, Merski C, Steindorf S, Wang S, Keller RW, Carlson JN. Neurochemical predisposition to self-administer morphine in rats. Brain Res. 1992;578(1–2):215–220. [PubMed: 1380861]

A

Week	Experiment Phase
0	Repeated Blast Injury
1	Handling
2	Jugular Catheterization Surgery
3	Food Self-Administration
4	Oxycodone Self-Administration (FR-2)
5	Oxycodone Self-Administration (FR-4)
6	Oxycodone Seeking
7	MRI

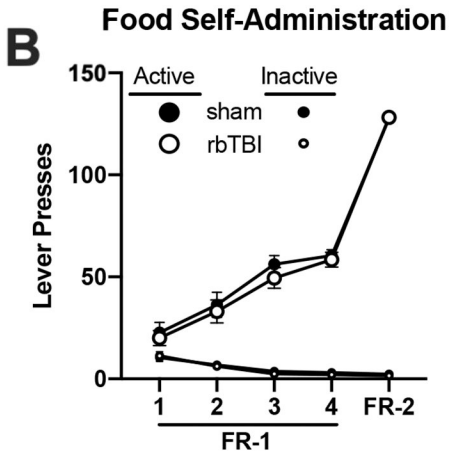

Figure 1:

A) Experimental timeline. B) Acquisition of food self-administration in sham and rbTBI rats. After rbTBI, rats underwent handling and jugular catherization. Following recovery, rats acquired sucrose self-administration without food restriction. Next, rats underwent oxycodone self-administration, then a seeking test under extinction conditions (no drug available), then had MRI one week later.

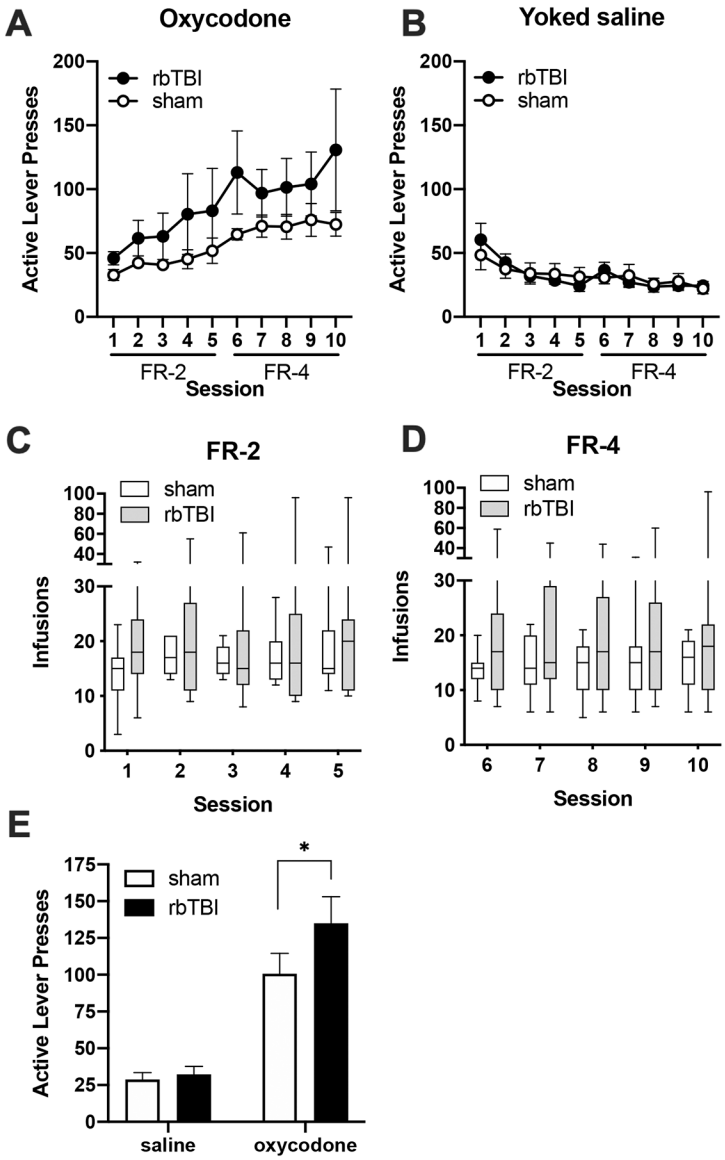

Figure 2:

Oxycodone self-administration and seeking. A) Active lever responses for oxycodone. B) Active lever responses in rats that received yoked saline infusions. C, D) Oxycodone infusions earned during FR-2 (C) and FR-4 (D) sessions. E) Active presses during extinction trial. Boxes represent median and quartiles, whiskers represent range. Bars represent mean +- SEM. *pÔëñ0.05.

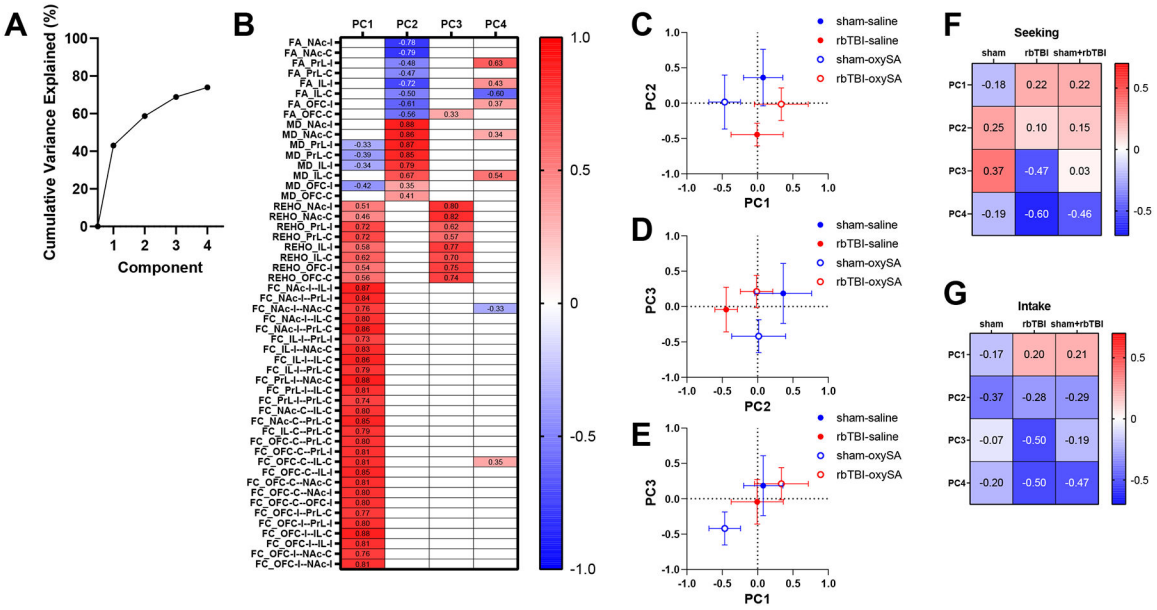

Figure 3:

Principal components analysis of MRI measures. A) Scree plot. B) Component loadings, C-E) Groups plotted against each pair of components 1–3 (plots with component 4 in Fig S1). F-G) Correlations between principal components seeking (PearsonÔÇÖs r, panel F) and oxycodone intake (SpearmanÔÇÖs rho, panel G). Symbols represent mean+-SEM. FA: fractional anisotropy, MD: mean diffusivity, REHO: regional homogeneity, FC: functional connectivity, PrL: prelimbic cortex, IL: infralimbic cortex, OFC: orbitofrontal cortex, NAc: nucleus accumbens. I, C: ipsi- or contra-lateral to injury, corresponding to left or right hemisphere, respectively in all rats.

A

FA v. Seeking		sham	rbTBI	sham+rbTBI
Ipsilateral	PrL	-0.34	-0.64	-0.53
	IL	-0.46	-0.46	-0.46
	OFC	0.19	-0.23	-0.16
	NAc	*0.30*	-0.42	*-0.19*
Contralateral	PrL	0.10	-0.03	-0.03
	IL	0.35	0.30	0.30
	OFC	0.27	-0.46	-0.16
	NAc	-0.26	-0.37	-0.26

B

MD v. Seeking		sham	rbTBI	sham+rbTBI
Ipsilateral	PrL	*0.42*	*-0.05*	*0.12*
	IL	*0.25*	*-0.12*	*0.02*
	OFC	*0.59*	*-0.07*	*-0.05*
	NAc	*0.10*	*-0.12*	*-0.01*
Contralateral	PrL	*0.03*	*-0.07*	*0.11*
	IL	*-0.10*	*-0.36*	*-0.16*
	OFC	*0.33*	*-0.11*	*0.08*
	NAc	*0.26*	*0.01*	*0.05*

C

FA v. Intake		sham	rbTBI	sham+rbTBI
Ipsilateral	PrL	-0.03	*-0.32*	*-0.31*
	IL	-0.48	*-0.36*	*-0.36*
	OFC	0.17	*-0.07*	*-0.12*
	NAc	*0.48*	*0.04*	*0.03*
Contralateral	PrL	0.15	*0.05*	*0.16*
	IL	0.39	*0.65*	*0.59*
	OFC	0.12	*-0.07*	*-0.05*
	NAc	0.11	*0.07*	*0.01*

D

MD v. Intake		sham	rbTBI	sham+rbTBI
Ipsilateral	PrL	*-0.03*	*-0.30*	*-0.19*
	IL	*-0.10*	*-0.67*	*-0.36*
	OFC	*0.73*	*-0.13*	*-0.04*
	NAc	*-0.27*	*-0.40*	*-0.31*
Contralateral	PrL	*-0.32*	*-0.29*	*-0.17*
	IL	*-0.15*	*-0.67*	*-0.55*
	OFC	*0.46*	*-0.36*	*-0.16*
	NAc	*-0.15*	*-0.52*	*-0.30*

Figure 4:

Correlations between structural neuroimaging measures and seeking or intake. FA: fractional anisotropy, MD: mean diffusivity, PrL: prelimbic cortex, IL: infralimbic cortex, OFC: orbitofrontal cortex, NAc: nucleus accumbens, Ipsilateral: left, contralateral: right. Italicized values represent Spearman’s rho instead of PearsonÔÇÖs r.

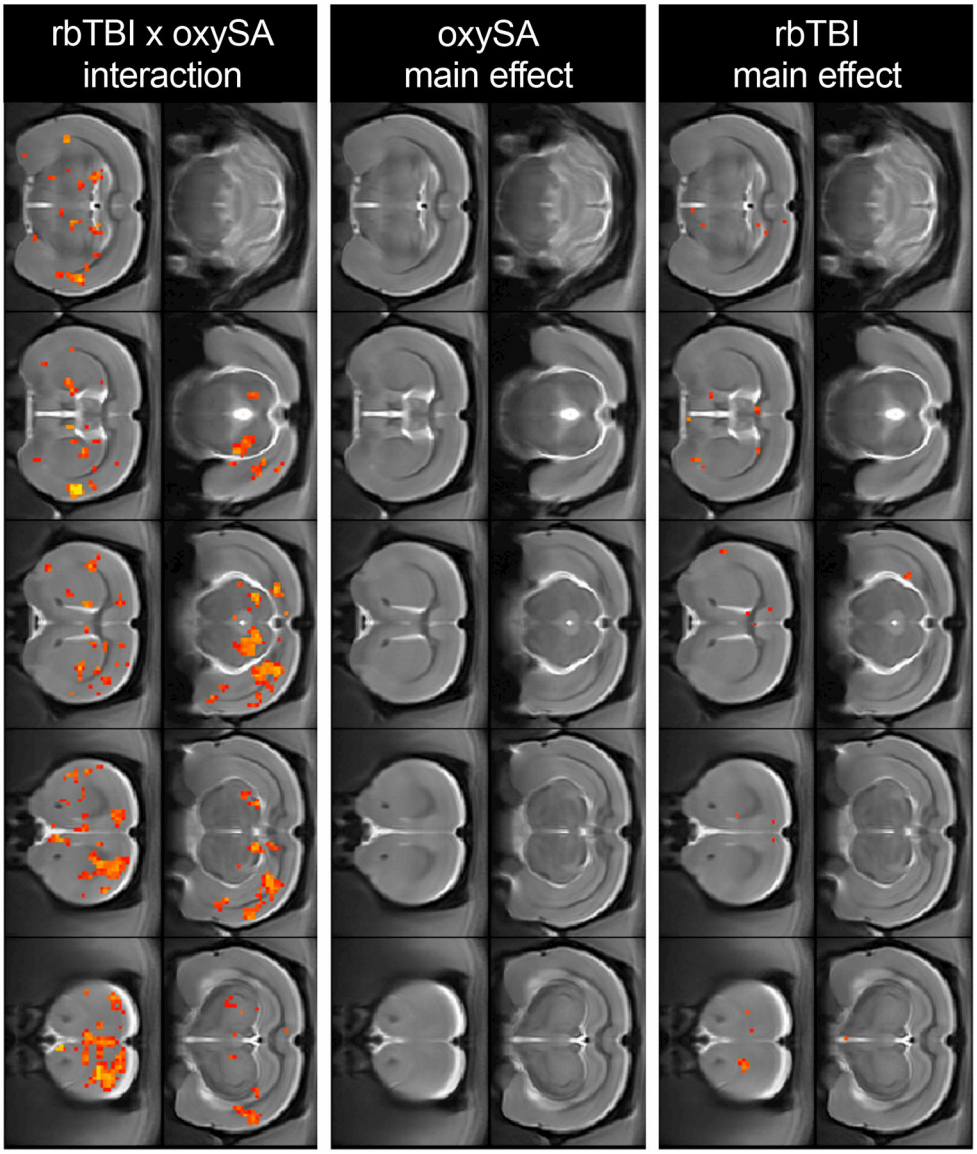

Figure 5:
Regional homogeneity (REHO) of BOLD signal. Red/yellow voxels represent main or interaction effects at pÔëñ0.05 (uncorrected).

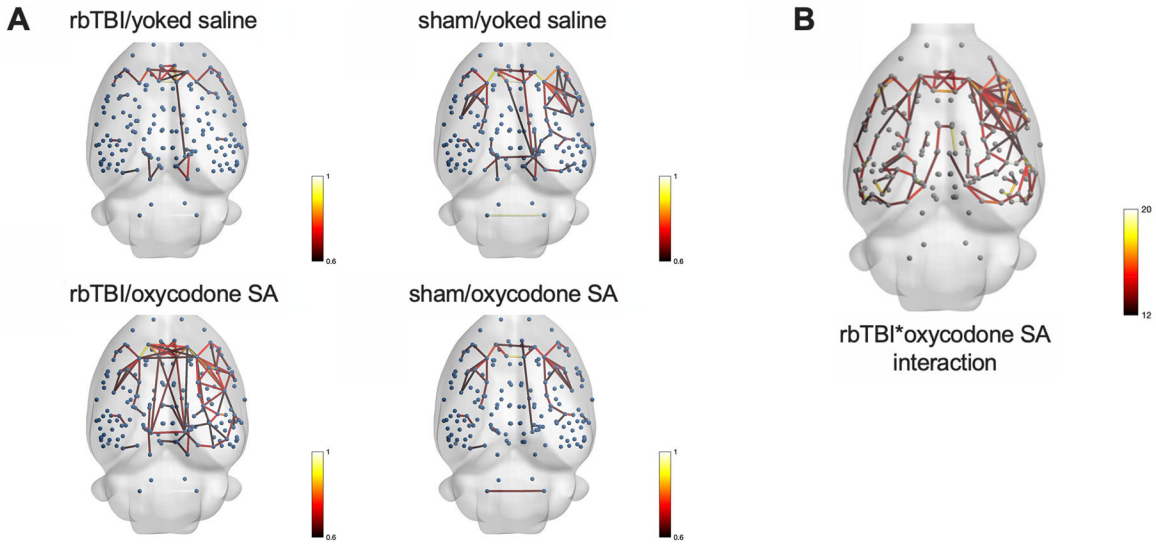

Figure 6:

NetworkÔÇÉbased statistics. A) Each node (blue sphere) represents a region of interest, each edge represents a significant correlation between nodes. B) Nodes connected by edges had a significant interaction between rbTBI and oxycodone self-administration. Edges are colored based on Pearson r values (A) or F values (B).

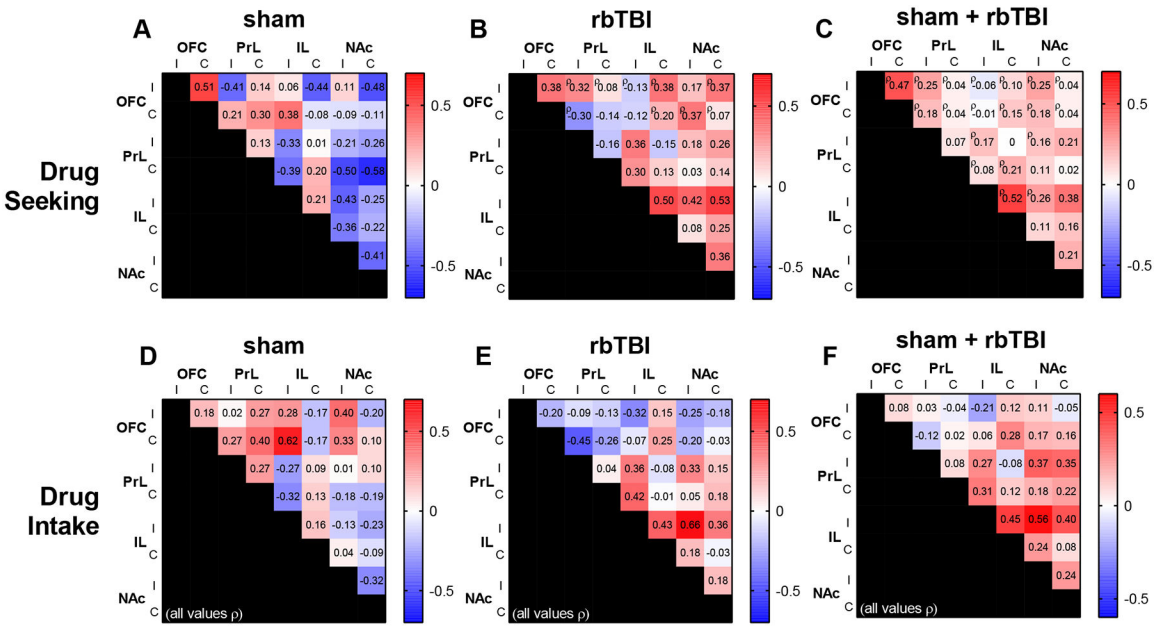

Figure 7:

Relationship between functional connectivity and drug seeking (A-C) or drug intake (D-F). Values are Pearson r except where denoted by ¤ü. I, C: ipsi- or contra-lateral to injury, corresponding to left or right hemisphere, respectively in all rats.